Scienxt Journal of Computer Science & Information Technology
2023; Volume-1; Issue-1, pp. 51-64

Examining the Effects of Material Dimensions on Flex-forming Process Wrinkling

Abhishek Gupta*[1], Rohit Yadav[2]

[1, 2] ***Department of Computer Science Engineering,***
Vaishno College of Engineering,
Bhadroya, Himachal Pradesh
E-mail: ***abhi.gupta@vaishno.edu.in***
https://www.zenodo.org/deposit/805671

*Corresponding author: Abhishek Gupta

Abstract:

The automotive and aerospace industries rely heavily on sheet metal forming as a key production process. Flexible production and the capacity to create several components at once make flex forming one of the most popular sheet metal forming methods. Wrinkling is a prevalent problem with convex-shaped flex-formed components, which is widespread in the industry. Predicting wrinkling before manufacturing is essential to reducing scrap rates, labour time, and other unforeseen expenditures. A flex-forming press was used to perform extensive trials with convex contoured pieces in order to study the influence of geometric factors on wrinkling. The findings reveal that when flange length, contour radius, and sheet thickness decrease, the likelihood to wrinkle rises. A wrinkling limit diagram is then generated from the testing results, which specifies safety and failure zones for various material conditions and sheet thicknesses. The schematics that have been created may be used to design components that are free of defects, decrease scrap, and lower manufacturing costs.

Keywords:

Flex forming; Sheet forming; Wrinkling; Convex contour flange

1. Introduction

The essential principle of the hydroforming process is the application of pressurized fluid to a sheet in order to create a portion. In general, pressurized fluid is utilized to produce the component, and a single die is often used [1]. During diaphragm formation (also known as flex forming), which is a specialized kind of hydroforming, a force is generated by pressurizing fluid in a closed circle fluid system, and this force is then utilized to create the sheet of metal [2]. During the process, the sheet metal is put onto a sheet metal die (often the lower die), with the diaphragm, which contains the fluid reservoir, positioned at the top of the die. The fluid is then compressed, and the diaphragm is pushed closer to the lower die as a result of the pressure. In this case, as you move the diaphragm, the sheet gets pushed between the diaphragm and the bottom die. Increased pressurization induces elastomeric diaphragm behavior similar to that of an upper die, with sheet metal being dragged into the lower die and the forming process being completed [3].

Due to the diaphragm's similarity to the top die, it is able to handle multiple component manufacturing. Because of this, it is possible to produce pieces with a variety of distinct forms. There are often a large number of unique components in the aircraft sector, each with a finite supply. As a result, this technique is frequently used and offers significant cost savings to the aerospace sector. The surface quality of flex formed pieces is superior to that of other techniques of production[4]. To make complicated and difficult-to-form pieces, hydraulic pressure is used rather of an upper die. Only one lower die is required in this process compared to a normal sheet metal forming operation that requires an upper and lower die set. Savings in labour costs and the removal of the higher die are the most significant benefits of this procedure [5]. Geometry with a near-net-shape is nearly there. Compared to the usual approach, the thickness thinning is lower and the thickness distribution is more uniform. When flex-forming convex-contoured components, the most prevalent failure mode is wrinkling, which often occurs on the part's flange. When the flange edge length is reduced after being formed, the maximum compression in the hoop direction takes place [6].

Using both experimental and computational methods, the influence of sheet thickness, die bend radius, flange length, and rolling direction on the flanging of AA2024-T3 components with straight and convex contours. They observed that the die radius and the rolling direction had no influence on the wrinkling, but the flange length and the sheet thickness do. Experimental and finite element findings were found to be very compatible [7]. Contour radius has an impact on wrinkling. Wrinkling is reduced when the radius of the contour is increased. A mathematical

model developed and demonstrates the connection between flange length and strain. As the flange lengthens, creases become more pronounced, as can be seen from the data. Finite element analysis to investigate the wrinkles that arise when rubber is used to produce convex-shaped pieces out of Ti-15-3 material [8]. The length of the flange and the kind of rubber used in the research were shown to affect wrinkling. Hydroforming wrinkles using both experimental and computational methods [9].

It was found that wrinkling was influenced by material stress and the diameter-to-thickness ratio of the pieces. Cryorolled AA5083 sheet material was studied hydro formingly. They discovered that hydroforming process produces more successful components with complicated geometries than traditional As shown in Wrinkling Limit Diagrams (WLDs), a wrinkle-free convex contoured flaring of AA2024-O and AA2024-W aluminium alloys has been created in this research [9]. This hasn't been thoroughly researched. Applications in the aircraft sector rely heavily on it. On the flex-forming press, wrinkling is studied as a function of sheet thickness, flange length, and contour radius. Predicting wrinkling and ensuring defect-free components are the goals [10].

2. Materials and Methods

2.1. Sheet materialproperties

Material qualities and geometric proportions have a role in wrinkling. The mechanical characteristics of AA2024 aluminium alloy were determined by conducting tensile tests at both O andWtemperatures. Each test was performed in a separate direction using a Zwick/Roell model Z100 machine with a deformation speed of 100mm/min [11]. Fig.1 depicts the real stress vs. true strain graphs for the two scenarios. List of mechanical parameters including elastic modulus, yield strength and ultimate tensile strengths are shown in Table-1 of the results of testing. Elongation, strength coefficient K and strain hardening exponent n. Fig.1 curves and Table-1's mechanical characteristics show that AA2024-W is more robust than AA2024-O. With increased sheet strength, convex contoured flanging has a greater propensity to wrinkle.

Table-1: The results of testing

Material	***E*[*GPa*]**	***YS*[*MPa*]**	***UTS*[*MPa*]**	□	***K*[*MPa*]**	***n***
AA2024-O	75	62	216	0.16	310	0.21
AA2024-W	75	148	423	0.18	710	0.26

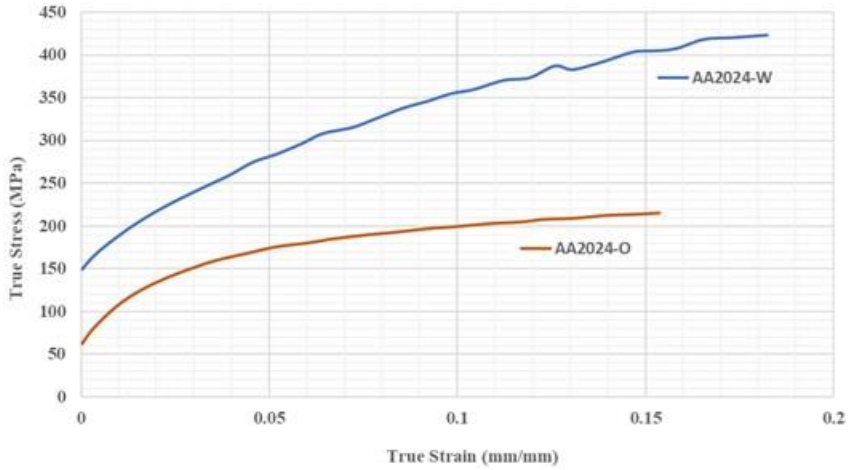

Figure.1: True stress Vs. true strain curves of AA2024-O and AA 2024-W

2.2. Experiments and setup

The purpose of experiments is to determine the effects of material and part geometry on wrinkling and establish a wrinkling.

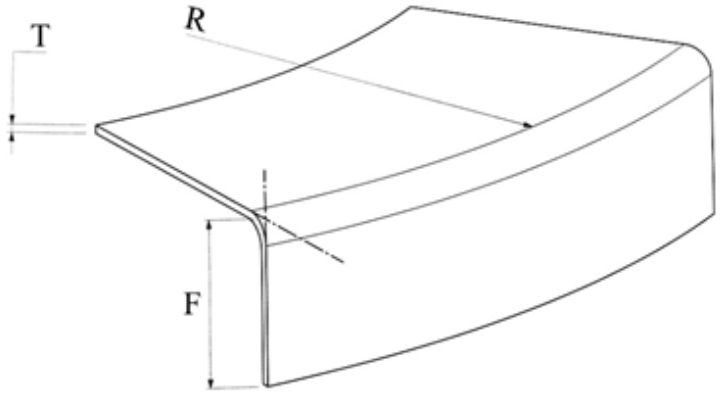

Figure. 2: Experimental parameters: sheet thickness (T), contour radius (R), and flange length (F)

As a result, wrinkling is more likely to develop in the -W- condition than in the -O- condition. As a result of its use in aviation component designs, the experimental parameters were selected to have the greatest impact on wrinkling [12]. Parts may be made in either O or W state with the most common being AA2024. As a result, criteria based on the experiments utilised both AA2024-O and AA2024-W. For example, in Fig. 2, you may see experimental characteristics such sheet thickness, contour radius, and flange length. Experiments are conducted with the same 6mm bend radius, which is known to have no influence on wrinkle formation. Table- 2 summarises the results for several experimental variables [12].

Table. 2: Experimental parameters and their values

Material Conditions	AA2024-O		AA2024-W		
Material thickness, T (mm)	0.63	1.27	1.60		2.00
Contour radius, R (mm)	125	250	500	1000	2000
Flange length, F (mm)	20		30		40
Bending radius (mm)	6.0				

Fig.3 depicts the experiment setup. A total of four thicknesses, five radii of curvature, and three flange lengths were evaluated with two distinct materials. The tests yielded a total of 120 specimens.

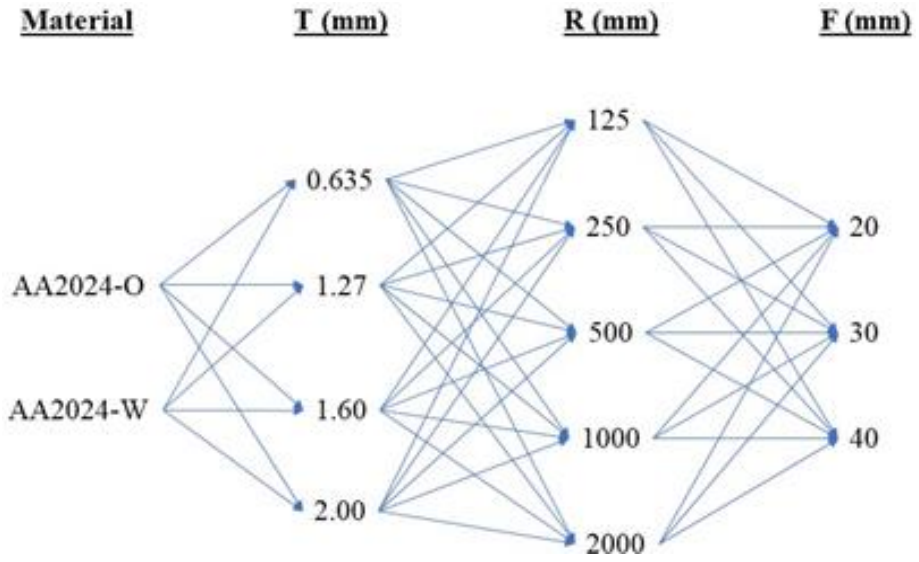

Figure. 3: Experiments configuration: sheet thickness (T), contour radius (R), and flange length (F)

Fig. 4(a) shows the experimental setup. The studies were conducted using a single die. In 24 cycles, this die was able to produce all possible configurations (2 material x 4 thickness x 3 flange length). Because high pressures prevent movement, the die is simply put into the tray of a flex forming press without being fixed in place. Guide pins connect specimens to this die so that they may be produced [13]. All studies were carried out at 70MPa forming pressure and 45°C oil temperature under 34 °C ambient conditions. The whole forming process took roughly three minutes, during which time the component was subjected to its maximum pressure for three seconds [14]. Fig. 4(b) depicts the finished products of the forming process.

Wrinkling defects have been found in several configurations with shifting numbers and sizes after completing studies. AA2024-W material, 1.27mm thickness, 125 mm contour radius, and

40mm flange length is one of those setups that results in two wrinkle forms (Fig. 5) [15].

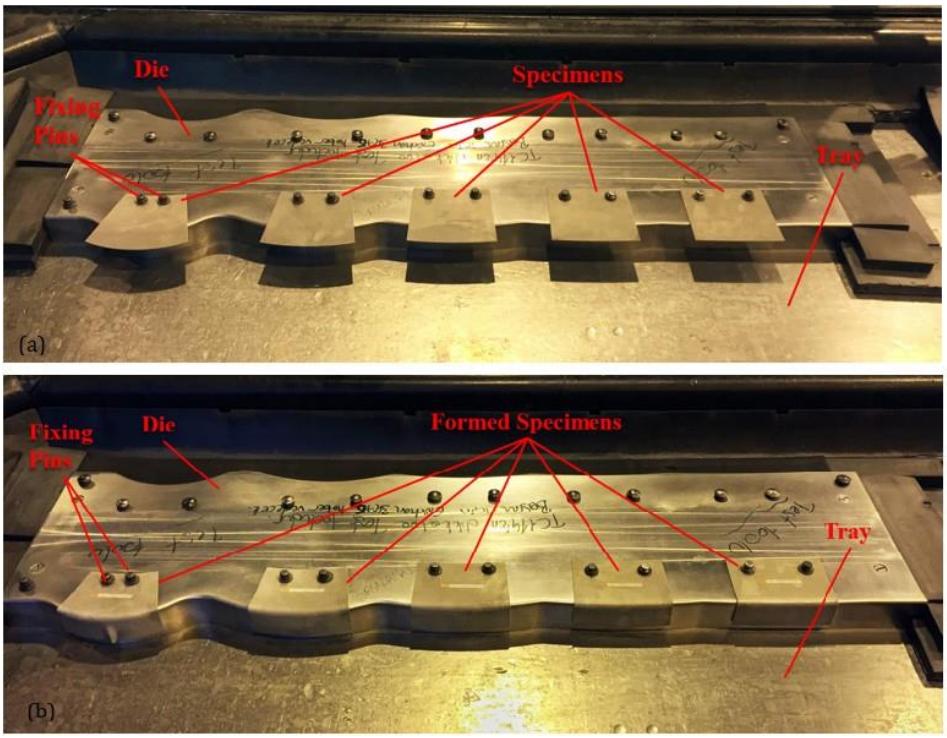

Figure. 4: Experimental Setup: a) Specimens are attached onto the die with fixing pins and the die is placed on the tray of the press b) Formed specimens on experimental setup.

Figure. 5: A formed specimen sample with wrinkling defect (material: AA2024-W, thickness: 1.27mm, contour radius: 125mm, flange length: 40mm).

The height and breadth of a wrinkle may be measured using two parameters: t and w. (Fig. 6). The wrinkle diameters were measured and recorded in Table 3 after the completion of the 24 runs. Because of the crushed nature of several samples, measurements could not be taken. Specimen flange edges were painted on plots in figure for better visualization. Those graphs clearly demonstrate the impact of experimental settings on wrinkle formation [11].

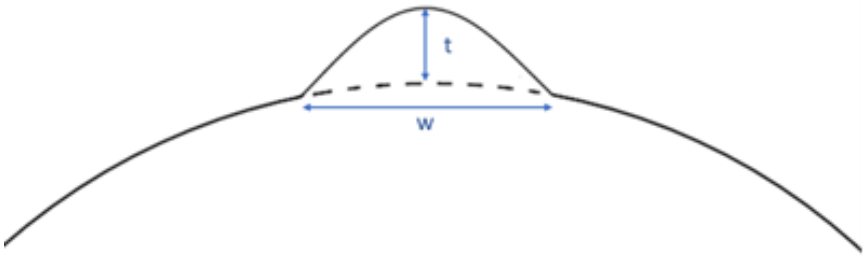

Figure. 6: Schematic view of wrinkle dimensions

Table-3: Wrinkling measurements

Experiment No	Material	T (mm)	R (mm)	F (mm)	Number of Wrinkles	t_1 x w_1 (mm)	t_2 x w_2 (mm)	t_3 x w_3 (mm)	t_4 x w_4 (mm)
1	AA2024-O	0.63	125	20	1	0.82 x 3.48	-	-	-
2	AA2024-O	0.63	125	30	2	2.55 x 3.18	2.42x 2.98	-	-
3	AA2024-O	0.63	250	30	1	1.05 x 3.62	-	-	-
4	AA2024-O	1.27	125	30	2	2.18 x 7.25	1.81x7.11	-	-
5	AA2024-O	1.60	125	30	1	1.28 x 7.39	-	-	-
6	AA2024-O	0.63	125	40	3	Not measured	1.7 x 3.88	1.09 x 3.74	-
7	AA2024-O	0.63	250	40	2	1.92 x 3.43	1.12 x 3.29	-	-
8	AA2024-O	0.63	500	40	1	0.58 x 2.93	-	-	-
9	AA2024-O	1.27	125	40	2	3.27 x 5.93	2.47 x 6.77	-	-
10	AA2024-O	1.60	125	40	2	0.34 x 4.04	0.31 x 2.96	-	-
11	AA2024-W	0.63	125	20	4	1.84 x 4.91	1.36 x 5.07	1.43 x 4.71	1.03 x 4.26
12	AA2024-W	1.27	125	20	1	2.77 x 8.79	-	-	-
13	AA2024-W	1.60	125	20	2	2.28 x 11.53	0.94 x 8.71	-	-
14	AA2024-W	2.00	125	20	1	1.89 x 16.37	-	-	-
15	Al2024-W	0.63	125	30	3	3.34 x 4.04	3.24 x 3.22	1.20 x	-

								4.44	
16	AA2024-W	0.63	250	30	2	2.33 x 4.21	1.26 x 4.48	-	-
17	AA2024-W	1.27	125	30	3	4.14 x 8.16	2.94 x 9.14	1.24 x 9.38	-
18	AA2024-W	1.60	125	30	1	5.67 x 9.63	-	-	-
19	AA2024-W	2.00	125	30	1	5.81 x 13.97	-	-	-
20	AA2024-W	0.63	125	40	2	4.18 x 2.97	3.77 x 4.42	-	-
21	AA2024-W	0.63	250	40	2	2.54 x 3.73	2.19 x 4.31	-	-
22	AA2024-W	0.63	500	40	1	1.69 x 4.07	-	-	-
23	AA2024-W	1.27	125	40	2	5.76 x 3.73	3.62 x 7.83	-	-
24	AA2024-W	1.27	250	40	1	3.32 x 8.16	-	-	-
25	AA2024-W	1.60	125	40	1	7.34 x 6.71	-	-	-
26	AA2024-W	1.60	250	40	1	2.19 x 10.75	-	-	-
27	AA2024-W	2.00	125	40	1	7.69 x 9.83	-	-	-

Fig. 7 depicts the wrinkling phenomenon in relation to sheet thickness. A thicker sheet will have less wrinkles but will also have larger wrinkles, which will ultimately fade. Thick structures withstand greater buckling than thin ones in the phenomenon of wrinkles.

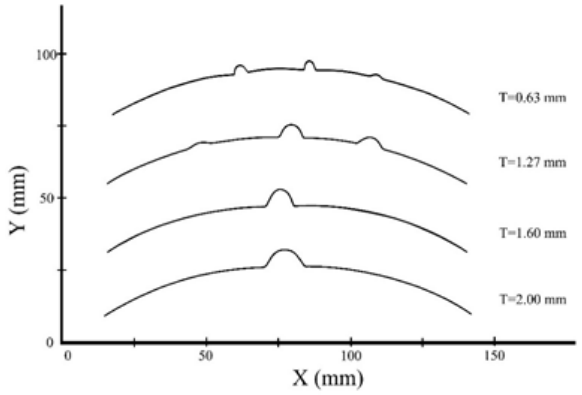

Figure.7: Effect of sheet thickness on wrinkling
(material: AA2024-W, flange length: 30mm, contour radius: 125mm

Fig.8 depicts the wrinkling impact of flange length. As the flange length rises, so does the

number of wrinkles. The arc length of the flange edge before and after shaping may be used to explain this tendency. The arc length of the flange edge was longer before forming, when the item was flat. The greater the flange length, the greater the amount of material that must be compressed into the final shape, resulting in more wrinkle development as a consequence.

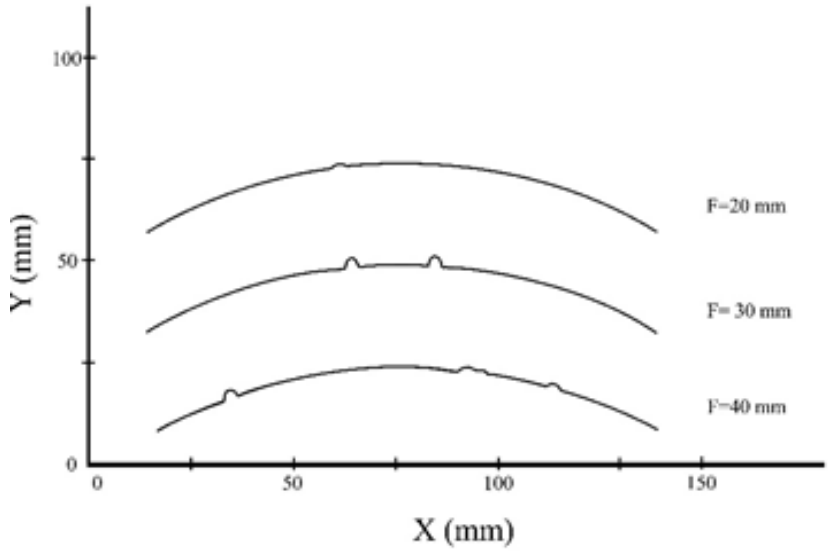

Figure. 8: Effect of flange length on wrinkling
(material: AA2024-O, thickness: 0.63mm, contour radius: 125mm)

Fig. 9 demonstrates how contour radius affects wrinkling. The severity of wrinkles reduces as the radius of the contour increases. This may be explained by looking back to the earlier discussion regarding the difference in arc length of the flange edge before and after the bends. As the radius of curvature increases, the effect diminishes until it reaches zero in straight bending, which is wrinkle-free.

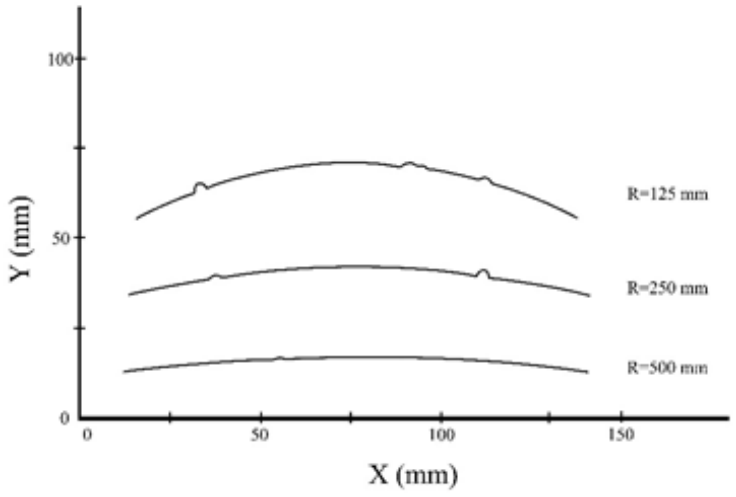

Figure. 9: Effect of contour radius on wrinkling
(material: AA2024-O, thickness: 0.63mm, flange length: 40mm

Fig.10 depicts the influence of temperature on wrinkling in AA2024 alloy. The stronger -W- state produces a prominent wrinkle, while the smoother -O- condition is devoid of wrinkles. Solution heat treatment hardens the material in the form of smaller grains, resulting in reduced mobility and an increased inclination to wrinkle. The wrinkling propensity rises with rising material strength, and flange length; and decreases with decreasing contour radius and sheet thickness, according to the data.

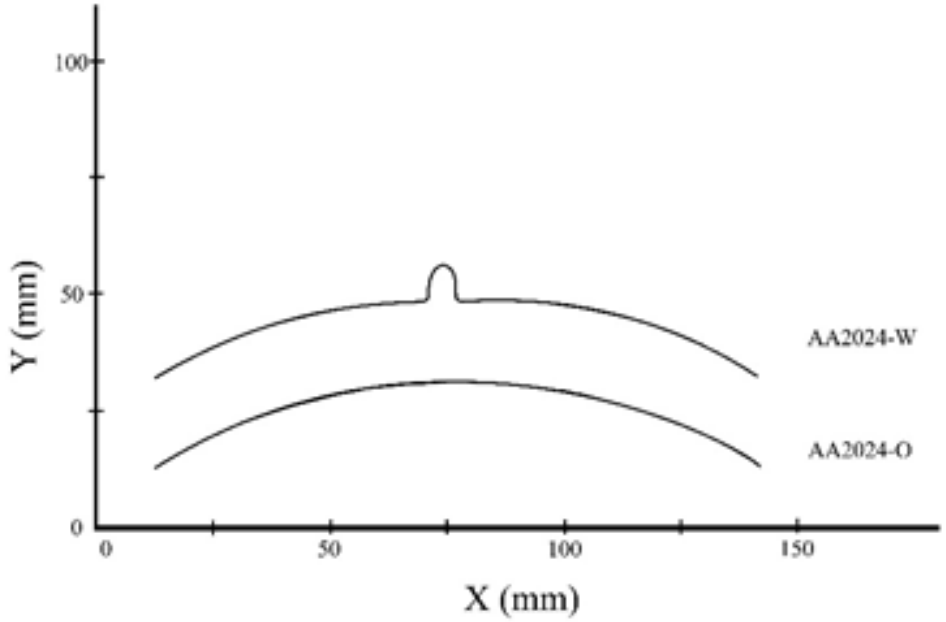

Figure. 10: Effect of alloy condition on wrinkling
(thickness: 1.60mm, flange length: 40mm, contour radius: 125mm)

To create a wrinkling limit, Wrinkling Limit Diagrams are used to evaluate experiment findings (WLD). For a particular geometry and material, these diagrams will show where the safety and failure zones are. AA2024-O 0.63 mm WLD is shown in Figure 11. The contour radius is represented by the abscissa, while the flange length is represented by the ordinate. Dots represent the outcomes of the experiments. It's possible to fit a wrinkling limit curve if those dots are categorised as wrinkled vs. wrinkleless. The area above and below this curve is known as the failure zone and the safety zone, respectively.

This curve could be defined mathematically as:

$$y = 14,427 \ln(x) - 49,658 \ldots\ldots \quad (1)$$

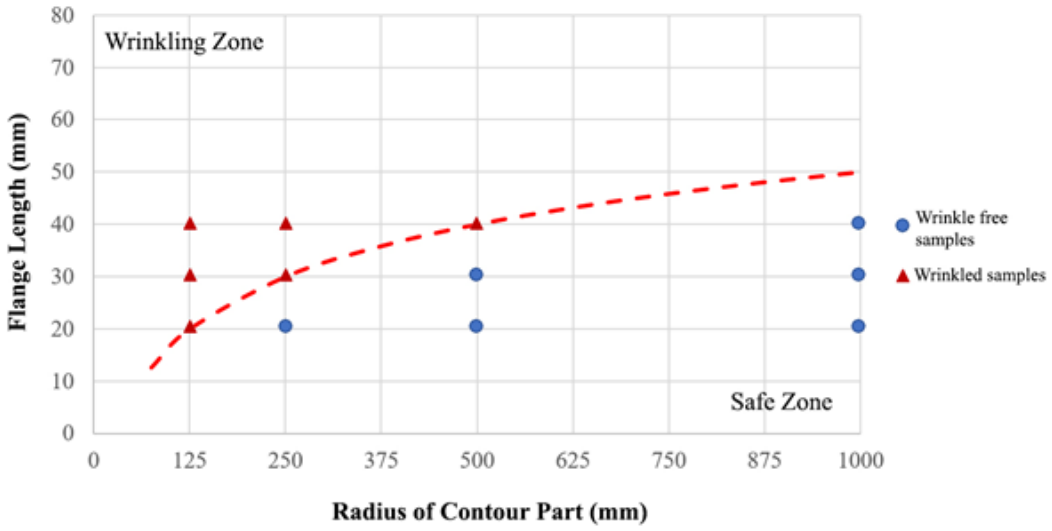

Figure. 11: Wrinkling Limit Diagram (WLD) for 0.63mm thickness AA2024-O

Wrinkling outcomes of various configurations may be discovered by using this equation, which is also applicable for configurations that were not found in the studies. All of the other materials and thicknesses had corresponding diagrams made.

3. Conclusion

Experiments were carried out on the wrinkling defect of convex-contoured pieces in the flex forming process. Experimental parameters included aluminum alloy conditions, sheet thicknesses, contour radiuses, and flange lengths. The following were the outcomes:

- Wrinkling was much reduced by the sheet's thickness. The propensity to wrinkle is considerably decreased when sheet thickness is raised.
- Another helpful parameter was the bend radius. Wrinkle sizes shrink as the radius of the contour increases, and finally vanish when the radius is expanded even more.
- The danger of material wrinkling grows as the length of the flange is extended.
- Wrinkling is also influenced by the material's elasticity. Wrinkling is more common in stronger fabrics.
- Wrinkle-free pieces may be produced by combining certain experimental settings. A curve separates the safety and failure zones in wrinkling limit diagrams based on these studies. The designer may utilize the wrinkling limit diagrams as a check tool at the conclusion of the process.

4. References

[1] C. Bell, J. Corney, N. Zuelli, and D. Savings, "A state of the art review of hydroforming technology: Its applications, research areas, history, and future in manufacturing," *Int. J. Mater. Form.*, vol. 13, no. 5, pp. 789–828, 2020.

[2] E. Kamil Hussein Abdulla Dhayea Assi and A. Hussein Kadhem, "INFLUENCES OF FRICTION CONDITIONS ON SHEET HYDROFORMING USED IN AUTOMOBILE INDUSTRIES Introduction," *Increasing Use Altern. Fuels Cem. Plants*, vol. 28, no. 1, pp. 2–22, 2015.

[3] O. M. Ikumapayi, E. T. Akinlabi, N. Madushele, and S. O. Fatoba, "A brief overview of bending operation in sheet metal forming," *Lect. Notes Mech. Eng.*, no. September, pp. 149–159, 2020.

[4] J. C. Williams and R. R. Boyer, "Opportunities and issues in the application of titanium alloys for aerospace components," *Metals (Basel).*, vol. 10, no. 6, 2020.

[5] S. Thiruvarudchelvan and F. W. Travis, "Hydraulic-pressure-enhanced cup-drawing processes - An appraisal," *J. Mater. Process. Technol.*, vol. 140, no. 1-3 SPEC., pp. 70–75, 2003.

[6] C. Liu, M. Li, and W. Fu, "Principles and apparatus of multi-point forming for sheet metal," *Int. J. Adv. Manuf. Technol.*, vol. 35, no. 11–12, pp. 1227–1233, 2008.

[7] H. A. Hatipoğlu, N. Polat, A. Koksal, and A. E. Tekkaya, "Modeling Flexforming (Fluid Cell Forming) Process with Finite Element Method," *Key Eng. Mater.*, vol. 344, pp. 469–476, 2007.

[8] Y. Dewang, M. S. Hora, and S. K. Panthi, "Prediction of crack location and propagation in stretch flanging process of aluminum alloy AA-5052 sheet using FEM simulation," *Trans. Nonferrous Met. Soc. China (English Ed.*, vol. 25, no. 7, pp. 2308–2320, 2015.

[9] S. B. Chikalthankar, G. D. Belurkar, and V. M. Nandedkar, "Factors Affecting on Springback in Sheet Metal Bending : A Review," *Int. J. Eng. Adv. Technol.*, vol. 3, no. 4, pp. 247–251, 2014.

[10] F. T. Feyissa and D. R. Kumar, "Enhancement of drawability of cryorolled AA5083 alloy sheets by hydroforming," *J. Mater. Res. Technol.*, vol. 8, no. 1, pp. 411–423, 2019.

[11] F. T. Feyissa and D. R. Kumar, "Enhancement of drawability of cryorolled AA5083 alloy sheets by hydroforming," *J. Mater. Res. Technol.*, vol. 8, no. 1, pp. 411–423, 2019.

[12] N. Liu, H. Yang, H. Li, and S. Yan, "Plastic wrinkling prediction in thin-walled part forming process: A review," *Chinese J. Aeronaut.*, vol. 29, no. 1, pp. 1–14, 2016.

[13] G. Winiarski, T. Bulzak, Ł. Wójcik, and M. Szala, "Numerical Analysis of a Six Stage Forging Process for Producing Hollow Flanged Parts from Tubular Blanks," *Adv. Sci. Technol. Res. J.*, vol. 14, no. 1, pp. 201–208, 2020.

[14] P. Gupta, A. Szekeres, and J. Jeswiet, "Manufacture of an aerospace component with hybrid incremental forming methodology," *Int. J. Mater. Form.*, vol. 14, no. 2, pp. 293–308, 2021.

[15] L. D. Bloom, J. Wang, and K. D. Potter, "Damage progression and defect sensitivity: An experimental study of representative wrinkles in tension," *Compos. Part B Eng.*, vol. 45, no. 1, pp. 449–458, 2013.

Cite as

Abhishek Gupta*, Rohit Yadav. (2023). Examining the Effects of Material Dimensions on Flex-forming Process Wrinkling. https://doi.org/10.5281/zenodo.8056732